Effect of acicular ferrite on banded structures in low-carbon microalloyed steel

Lei Shi, Ze-sheng Yan, Yong-chang Liu, Xu Yang, Cheng Zhang, and Hui-jun Li

State Key Laboratory of Hydraulic Engineering Simulation and Safety, School of Materials Science and Engineering, Tianjin University, Tianjin 300072, China

Abstract: The effect of acicular ferrite (AF) on banded structures in low-carbon microalloyed steel with Mn segregation during both isothermal transformation and continuous cooling processes was studied by dilatometry and microscopic observation. With respect to the isothermal transformation process, the specimen isothermed at 550°C consisted of AF in Mn-poor bands and martensite in Mn-rich bands, whereas the specimen isothermed at 450°C exhibited two different morphologies of AF that appeared as bands. At a continuous cooling rate in the range of 4 to 50°C/s, a mixture of AF and martensite formed in both segregated bands, and the volume fraction of martensite in Mn-rich bands was always higher than that in Mn-poor bands. An increased cooling rate resulted in a decrease in the difference of martensite volume fraction between Mn-rich and Mn-poor bands and thereby leaded to less distinct microstructural banding. The results show that Mn segregation and cooling rate strongly affect the formation of AF-containing banded structures. The formation mechanism of microstructural banding was also discussed.

Keywords: low-carbon microalloyed steel; acicular ferrite; microstructure; manganese; segregation

1. Introduction

For the last three decades, low-carbon microalloyed steel has been extensively used in pipeline structures, the automotive industry, and the construction of bridges and ships [1–2]. The steel has a good combination of high strength, improved toughness, and formability, which can be controlled through a reasonable combination of chemical composition, thermomechanical control processing (TMCP), and an accelerated cooling process. A typical microstructure of microalloyed steel is acicular ferrite (AF). AF is defined as the absence of carbides, non-equiaxed ferrite plates, and martensite/austenite (M/A) constituents between ferrite crystals and is formed in the intermediate temperature range via a displacive mechanism of phase transformations. AF has been widely reported to nucleate at non-metallic inclusions within the austenite grains and to grow in various directions. It can effectively improve the toughness because of its fine interlocking microstructure [3–5]. Alloying elements such as Mn, Mo, Cr, Ni, and Nb are added to steel to im-

prove the strength of steel through various strengthening mechanisms [6–7]. However, the addition of substitutional alloying elements and hot rolling can result in the presence of banded structures, which is detrimental to the mechanical properties of steel because of strain anisotropy [8].

Banded structures have been recognized for many years as a well-known phenomenon in hot-rolled steel [9–12]. The underlying cause of banding is chemical segregation of substitutional alloying elements. The dendritic growth mode of steel during solidification always produces interdendritic regions of high solute concentration, and these regions are aligned with the deformation direction during subsequent rolling [13]. Microstructural inhomogeneities can cause the anisotropy in the mechanical properties of steel because cracking is prone to propagation along microstructural bands [14]. Thus, band prevention greatly improves the mechanical properties of steel. Previous investigations have suggested that the presence of bands can be prevented by increasing the cooling rate or the austenite grain size, despite the uneconomical feasibility of these measures in industry [10,15].

Corresponding author: Yong-chang Liu   E-mail: licmtju@163.com

🐦 Springer

A common type of banded microstructure is alternating parallel bands of ferrite and pearlite, which often occur in slowly-cooled plain carbon steel. Manganese (Mn) is widely accepted as one of the determing componets which bring the formation of banding structures [10]. Mn is a strong austenite stabilizer that can lower the Ar_3 temperature. Therefore, ferrite first nucleates in Mn-poor bands with a higher Ar_3 temperature at a lower cooling rate and rejects carbon into neighboring Mn-rich regions. Eventually, pearlite will form in Mn-rich bands [15].

Intense research has conducted to study the quantification of the degree of ferrite/pearlite bands [16–17], the influence of banded structures on overall mechanical properties [14], and some methods of effectively preventing banding [18], although conventionally hot-rolled ferrite/pearlite steel is not widely used in the modern steel industry because of its poor mechanical properties. AF-dominated microstructures are well known to exhibit optimized mechanical properties. Although the formation of AF-containing banded microstructures is not as severe compared to the formation of ferrite/pearlite bands [19], they are unavoidable in microalloyed steel. However, most publications on microstructural banding have been based on ferrite/pearlite bands alone, whereas the literature contains little work on AF-containing bands and their formation behaviors.

This study presents the characteristics of a series of various AF-containing banded structures under isothermal treatment and continuous cooling through dilatometry; their transformation behaviors are also investigated. The present work is designed to provide further insights into the formation mechanism of AF-containing bands.

2. Experimental

Low-carbon Mn–Mo–Nb microalloyed steel supplied as a hot-roll plate was used for experimental study. The chemical composition of the steel is given in Table 1. The microstructure of the as-received steel is shown in Fig. 1(a); it consists of banded ferrite (F) and pearlite (P). The Mn-concentration map measured using an electron probe micro-analyzer (EPMA) is presented in Fig. 1(b). As expected, the steel contained Mn-segregated bands parallel to the rolling direction; in addition, the microchemical band spacing of this steel was observed to be approximately 20 μm. The Mn-poor bands (level value: 1–14; the unit is X-ray counts) were composed of ferrite, and Mn-rich bands (level value: 16–32) were composed of pearlite. The local Mn concentrations were estimated to vary between approximately 0.7wt% (Mn-poor bands) and 1.3wt% (Mn-rich bands).

Table 1.   Chemical composition of the steel   wt%

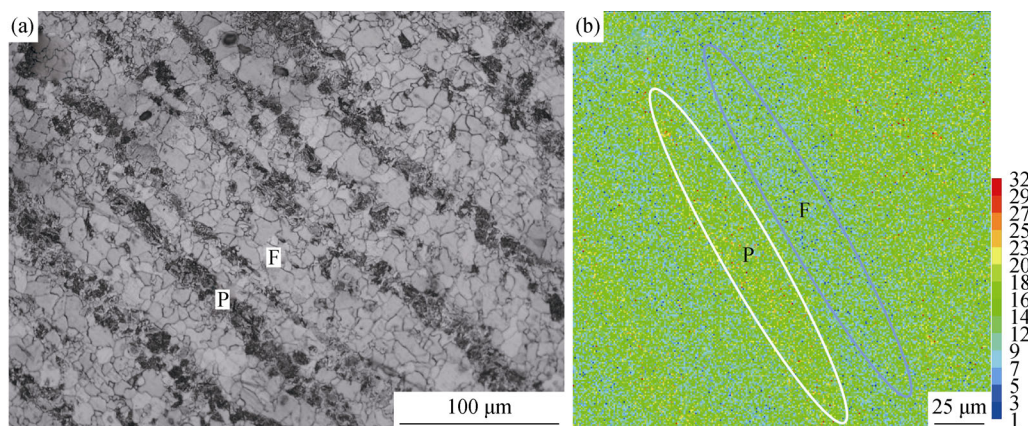| C	Mn	Si	Mo	Nb	Ni	Cr	Cu	N
0.13	1.06	0.41	0.33	0.02	1.22	0.26	0.66	0.0078

Fig. 1.   (a) Microstructure of the as-received steel; (b) Mn-concentration map showing segregated bands.

All heat treatments in this work were conducted on a high-resolution dilatometer (Bähr DIL805A/D). The diameter and length of the cylindrical samples for dilatometry were 5 mm and 10 mm, respectively. During isothermal holding (Fig. 2(a)), the samples were first austenitized at 900°C for 10 min, cooled rapidly to an isothermal temperature of 550 or 450°C, and then maintained at the isothermal temperature for 20 min. When the isothermal transformation was completed, the specimens were quenched to room temperature. During continuous cooling (Fig. 2(b)), the samples were austenitized at 900°C for 10 min, and then cooled to room temperature at a cooling rate of 0.1, 0.2, 0.5, 1, 2, 4, 8, 15, 30, 50, or 100°C/s.

A combination of optical microscopy (Olympus GX51) and transmission electron microscopy (TEM, JEM-100CX II) was used to determine the microstructures of specimens.

For optical microstructures, the specimens were mechanically polished and etched with a 4% nital solution. For TEM analysis, the specimens were sliced to a thickness of 300 μm, mechanically thinned to 50 μm, and then electro-

polished in a twin-jet polisher using a solution of 95vol% ethanol solution and 5vol% perchloric acid. In addition, the distribution of Mn in segregated bands was confirmed using EPMA.
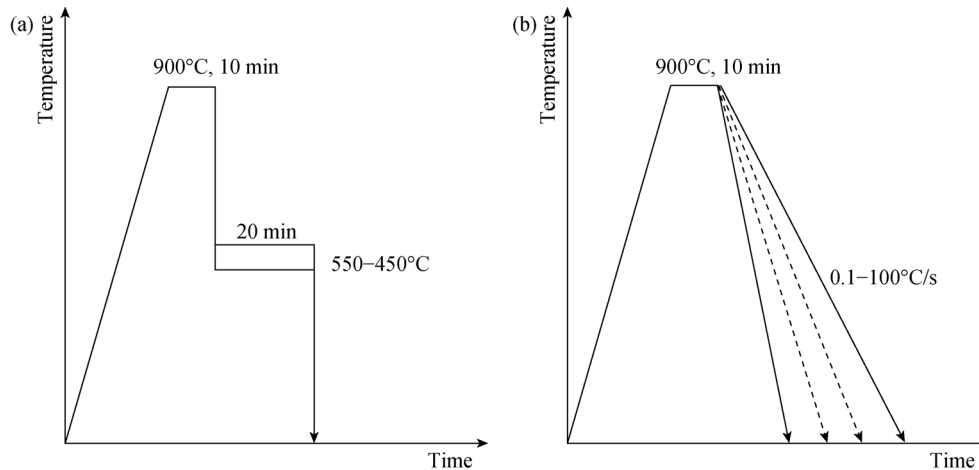

Fig. 2.   Schematic illustration of heat treatments: (a) isothermal holding; (b) continuous cooling.

3. Results

3.1. Banded structure during isothermal holding

The dilatation curves of specimens after isothermal transformation at 550 and 450°C are shown in Fig. 3. The curve of the specimen maintained at 550°C exhibits two distinct dilatational changes. The vertical part in the intermediate temperature range undoubtedly represents the AF transformation, and the dilatational change at low temperature corresponds to the martensite (M) transformation. However, in the case of the specimen maintained at 450°C, the dilatometric curve shows only one dilatational change at intermediate temperature, which means only the AF transformation occurred.
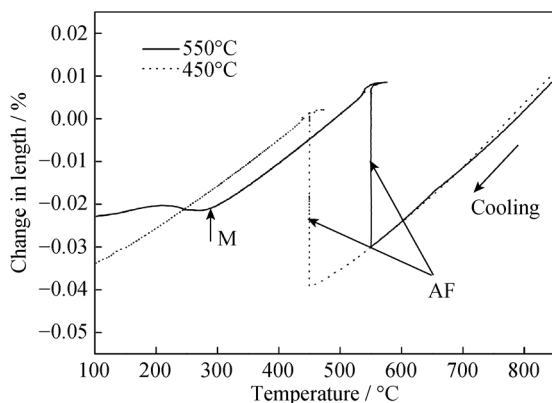

Fig. 3.   Temperature–dilatation curves of specimens after being isothermally maintained at 550°C and 450°C.

The corresponding optical micrographs of the specimens are shown in Fig. 4. The specimen maintained at an iso-

thermal temperature of 550°C (Fig. 4(a)) exhibits a banded microstructure of AF and martensite, both of which originated by displacive transformation of austenite. The AF apparently formed during the isothermal holding period, and the remaining austenite transformed to martensite after quenching. We observed that the Mn-poor regions correspond to AF, whereas martensite was formed in the Mn-rich regions, which means that the formation of AF is strongly related to Mn segregation. Although the AF is always accompanied by the formation of martensite/austenite constituents (M/A), the distribution and morphology of the band-like martensite differ significantly from those of M/A. Fig. 5 shows a representative TEM micrograph of the sample isothermally annealed at 550°C. Band-like martensite (M) clearly shows a conventional lath structure with high-density dislocations (Fig. 5(a)); however, this morphology is not observed in M/A (Fig. 5(b)). In addition, the grain size of the band-like martensite is approximately 5 μm, which is much larger than that of M/A (less than 1 μm). Most importantly, the distribution of M/A is dispersive within the AF matrix, while martensite is located along the bands. The aforementioned differences between martensite and M/A imply that their formation mechanisms differ substantially. Carbon partitioning during the growth of AF leads to the formation of M/A, whereas Mn segregation can result in band-like martensite; the reasons for this behavior will be discussed later. For a specimen isothermally held at 450°C, two different morphologies of AF appear as bands in the microstructure, as demonstrated in Fig. 4(b). AF plates in the Mn-rich bands become much finer in comparison to the Mn-poor bands.
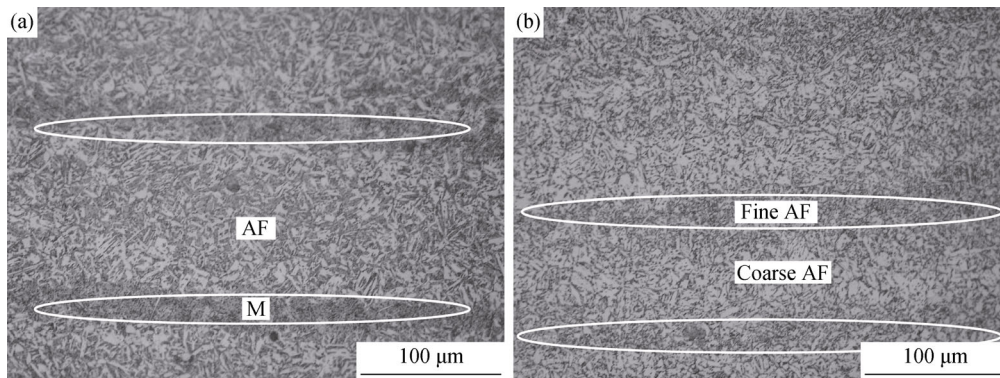
Fig. 4.   Optical micrographs of specimens after being isothermally maintained at 550°C (a) and 450°C (b) (the Mn concentration is greater in the regions indicated by white ovals).
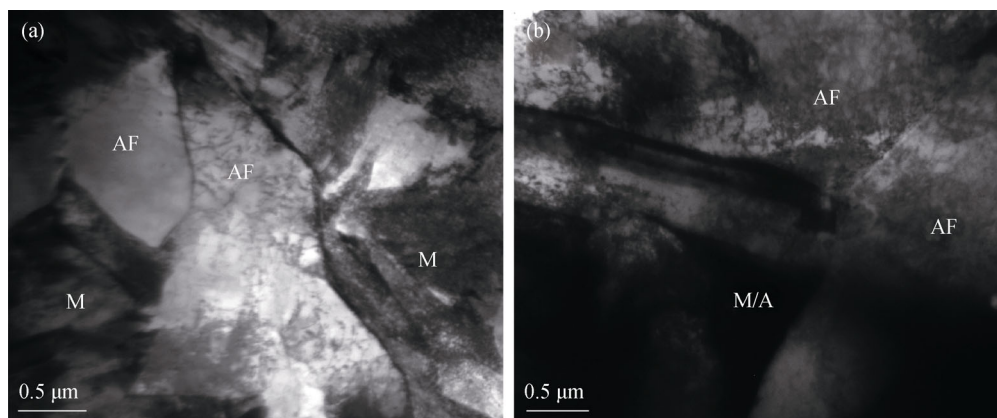

Fig. 5.   TEM micrographs of specimens maintained at 550°C for 20 min showing AF plates and lath martensite (a) and M/A constituents between AF plates (b).

The evolution of the volume fraction of AF as a function of isothermal holding time at 550 and 450°C, as obtained by the change in relative length observed by dilatometry, is given in Fig. 6. In the case of isothermal treatment at 550°C, the AF transformation reaches a stasis after the holding time of 621 s, and the resulting AF fraction is approximately 73%. The reason for this stasis is explained by the incomplete transformation phenomenon. However, in the case of isothermal treatment at 450°C, super-cooled austenite can completely transform to AF, and no incomplete transformation phenomenon occurs.

3.2. Development of a banded structure during continuous cooling

The continuous cooling transformation (CCT) diagram of experimental steel based on the dilatometric results and microstructural observations is presented in Fig. 7. As evident in the figure, the CCT diagram is characterized by multi-transformation curves, which indicates that complex transformation products that include polygonal ferrite, pearlite, AF, and martensite are obtained, depending on the cooling rate. Polygonal ferrite is avoided when the cooling rate exceeds 2°C/s. Pearlite is formed in the cooling rate range of 0.1–0.5°C/s. AF transformation occurs at cooling rates from 1 to 50°C/s. At rates greater than 4°C/s, martensite transformation is observed.
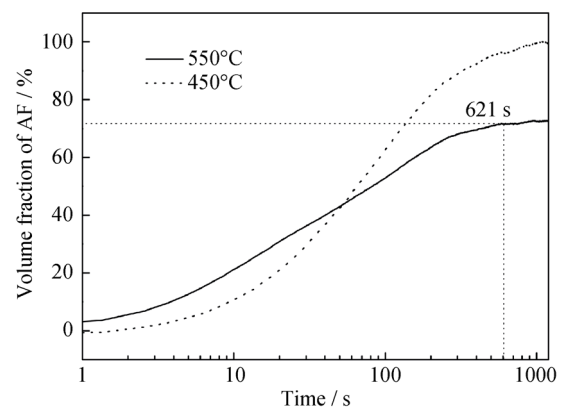

Fig. 6.   Effect of isothermal holding temperature on the volume fraction of AF.
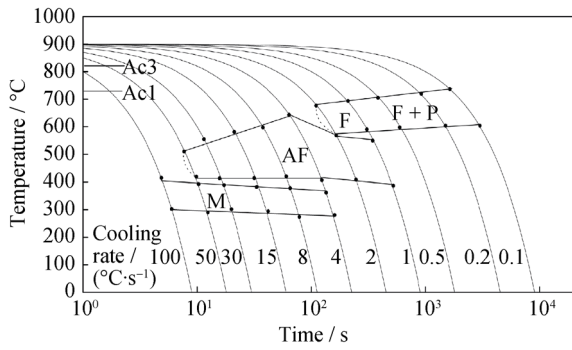
Fig. 7.   CCT diagram of experimental steel: F—polygonal ferrite; P—pearlite; AF—acicular ferrite; M—martensite.

Optical micrographs of the specimens during continuous cooling are shown in Fig. 8. The banded structure exhibits a complex variation at different cooling rates. At very low cooling rates (0.1–0.5°C/s), the microstructures (Figs. 8(a) and 8(b)) consist of alternating bands of ferrite and pearlite (F/P). At cooling rates of 1–2°C/s (Figs. 8(c) and 8(d)), pearlite formation is suppressed by the increased cooling rates and AF bands will form during cooling in the Mn-rich regions previously occupied by pearlite. Thus, F/AF bands are observed. Remarkably, the specimen cooled at 2°C/s exhibits much less pronounced banding.
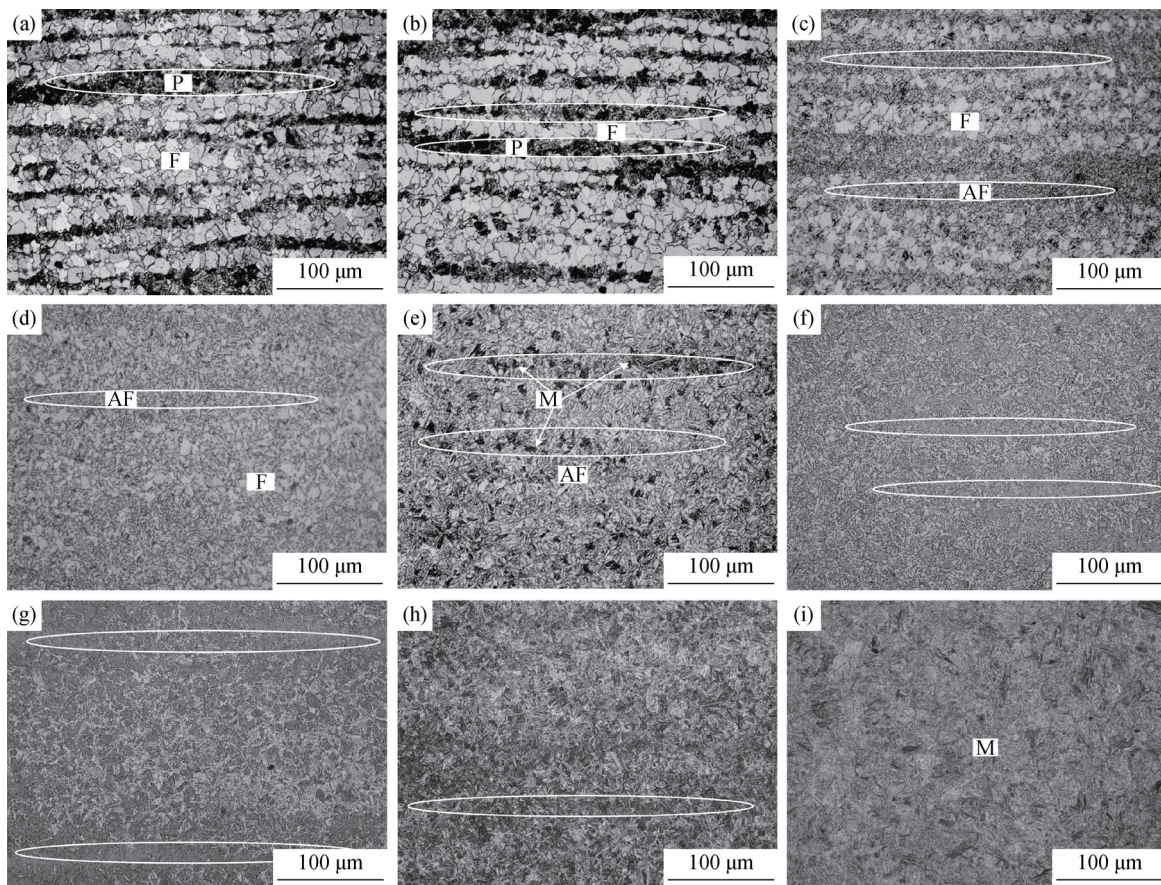

Fig. 8.   Optical micrographs of specimens continuously cooled at 0.1°C/s (a), 0.5°C/s (b), 1°C/s (c), 2°C/s (d), 4°C/s (e), 8°C/s (f), 15°C/s (g), 50°C/s (h), and 100°C/s (i) (the Mn concentration is higher in the regions indicated by white ovals).

At higher cooling rates (4–50°C/s), the specimens (Figs. 8(e)–8(h)) exhibit a mixture of AF and martensite in both segregated bands, although the degree of banding differs. Fig. 9 shows the effect of cooling rate on the volume fraction of martensite in different Mn-concentration regions and the martensite volume ratio (R_m) between Mn-rich regions (Mn level value: 16–32) and Mn-poor regions (Mn level value: 1–14). The martensite fraction ratio, R_m, is determined from the following equation:

$$R_m = V_{rich} / V_{poor} \tag{1}$$

where V_{rich} and V_{poor} are the martensite volume fractions of Mn-rich and Mn-poor regions, respectively. The fraction of martensite in different Mn-concentration bands was measured from 10 optical micrographs of specimens subjected to each heat-treatment temperature, and the corresponding Mn content was confirmed by EPMA. For a given cooling rate, the martensite fraction in Mn-rich bands is clearly higher than that in Mn-poor bands, as shown in Fig. 9(a). Using an

optical microscope (Figs. 8(e)–8(h)), we noted that, compared to Mn-poor bands, the Mn-rich bands (indicated by white ovals) etch darker because of their greater martensite content. As the cooling rate is increased, the volume fraction of martensite increases in Mn-rich bands as well as in Mn-poor bands, although the martensite fraction in Mn-rich bands is still greater than that in Mn-poor bands. Moreover, as clearly indicated in Fig. 9(b), R_m decreases with increasing cooling rate, which means that the difference in martensite fraction between the Mn-rich and Mn-poor bands becomes smaller with the increasing cooling rate; i.e., a high
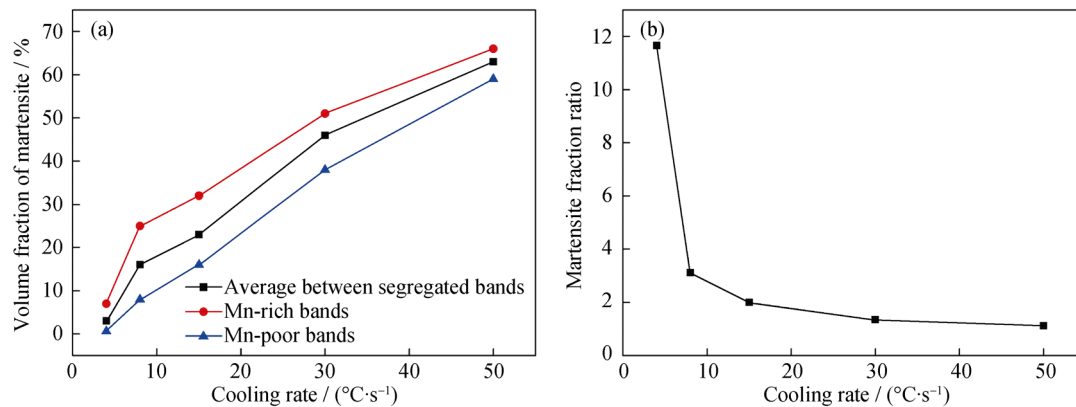
cooling rate can suppress the formation of banded structures. In particular, the volume fraction of martensite in the specimen cooled at 4°C/s (Fig. 8(e)) is very low (less than 4%); however, this martensite is almost entirely located in Mn-rich bands. When the cooling rate is increased to 50°C/s (Fig. 8(h)), the martensite fractions in Mn-rich and Mn-poor bands are very similar. Thus, the specimen cooled at 50°C/s exhibits a more homogeneous microstructure. At the highest cooling rate of 100°C/s (Fig. 8(i)), the microstructure comprises a fully martensite structure, and microstructural banding completely disappears.

Fig. 9. **Effect of the cooling rate on the volume fraction of martensite in regions with different Mn concentrations (a) and the martensite volume ratio (R_m) between Mn-rich regions and Mn-poor regions (b).**

4. Discussion

4.1. Incomplete transformation phenomenon and formation mechanism of AF-containing banded structures during isothermal holding

When the specimen is isothermally maintained at 550°C, the AF transformation exhibits an incomplete characteristic. As shown in Fig. 6, the super-cooled austenite cannot completely transform to AF. In principle, this transformation stasis behavior can be explained in terms of the displacive growth of AF subunits [20]. Carbon will partition into the residual austenite after the initial AF formation during the holding period, and carbide precipitation from austenite will be inhibited. Thus, the AF transformation can be expected to cease when the carbon concentration in the austenite reaches a critical value, the magnitude of which would be near the T_0 curve [20]. The residual austenite with a higher carbon content will remain stable or transform to martensite (M/A) during subsequent quenching. However, in the present study, extra attention was devoted to the morphology of untransformed austenite (martensite). The results clearly indicate that, if the incomplete transformation phenomenon in the sample isothermally transformed at 550°C is mainly attributed to carbon partitioning, then the distribution of martensite should be dispersive rather than banded within the AF matrix. AF plates grow out in more random directions by displacive transformation and do not partition the ejected C atoms in the proper direction with respect to Mn-rich bands. Thus, the presence of Mn-rich martensite bands in the microstructure formed at 550°C suggests that carbon partitioning does not strongly influence the transformation stasis, although untransformed austenite is associated with a somewhat higher carbon concentration.

We hypothesize that, in comparison with carbon segregation, Mn segregation is the predominant factor governing the incomplete transformation phenomenon in the present steel. As a strong austenite stabilizer, Mn significantly retards AF transformation and leads to a decrease in the start temperature of AF transformation (AF_s) [21]. Consequently, the AF_s of Mn-rich bands will be much lower than that of Mn-poor bands during the isothermal holding period. The lower AF_s of Mn-rich bands means that austenite in Mn-poor regions will transform to AF but austenite in Mn-rich regions will be stable at 550°C, thereby resulting in the incomplete transformation phenomenon and the formation of martensite bands. As the temperature is decreased to 450°C, no incomplete transformation phenomenon is observed because a lower isothermal temperature is associated

with the greater undercooling and driving force [22], which permits AF to form even in Mn-rich regions. Moreover, as is clearly evident in Fig. 4(b), Mn not only affects the AF transformation kinetics, but also modifies the morphology of AF. For the same isothermal temperature of 450°C, the AF in Mn-rich bands has a finer grain size, whereas Mn-poor bands exhibit coarse AF grains because Mn enrichment can suppress the growth of AF grains.

4.2. Effect of cooling rate on AF-containing banded structures

When the cooling rates are very low (0.1–0.5°C/s), ferrite will preferentially form at the Mn-poor layer, which leads to a higher Mn concentration in pearlite. Moreover, the addition of Mn can cause a shift of ferrite/pearlite-forming temperatures to the right side in the CCT diagram; thus, AF transformation is expanded to lower cooling rates in Mn-rich regions. This phenomenon explains the observations of specimens cooled at 1–2°C/s, where Mn-poor bands were observed to correspond to ferrite and Mn-rich bands were observed to correspond to AF. Furthermore, banded structures at a cooling rate of 2°C/s become less severe because of the higher cooling rate. Many previous studies have reported that a greater cooling rate can suppress the formation of band-like ferrite because accelerated cooling can cause less difference in the Ar$_3$ temperature and in the ferrite nucleation rate between Mn-rich and Mn-poor bands [10].

At cooling rates greater than 4°C/s, the formation of ferrite is totally suppressed. According to the CCT diagram, AF and martensite will exist together in the microstructure over a wide range of cooling rates: from 4 to 50°C/s. We observed that the amount of AF in Mn-poor bands is greater than that in Mn-rich bands. AF is known to intragranularly nucleate at inclusions within the austenite grains [18]. The lath-like AF that forms at higher temperatures divides the prior austenite into smaller regions. Subsequently, martensite will be restricted to form with decreasing temperature in these areas; i.e., the prior formed AF grains can stop the growth of martensite packets in the subsequent stage [23]. Therefore, for a given cooling rate, less AF is formed in Mn-rich bands because an increase in the Mn concentration reduces the formation temperature of AF and its growth rate, thereby inhibiting AF formation. Mn enrichment can also promote the formation of martensite, and vice versa [22,24], as schematically illustrated in Fig. 10.

In addition to the Mn content, AF formation also depends on the cooling rate [25]. Fig. 11 shows the fractions of AF and martensite as a function of temperature with different cooling rates (4–100°C/s). With an increase in cooling rate,

the start temperature of AF transformation (AF$_s$) apparently decreases and less AF is formed. The optimum cooling rate to form AF is 4°C/s, above which AF formation is suppressed by the increased rate because of the larger driving force for AF transformation at high rates. Thus, the accelerated cooling rate promotes the martensite transformation and enhances the hardenability. Moreover, the increased cooling rate can lead to a less distinct banded structure, as shown in Fig. 9(b). The accelerated cooling causing a less difference in AF nucleation rate in both segregated bands is reasonable. When the cooling rate is higher, the effect of Mn concentration on AF nucleation starts to decrease, and the AF fraction in Mn-rich and Mn-poor regions becomes similar. Eventually, when the cooling rate is sufficiently high (100°C/s) to entirely inhibit AF formation in both Mn-rich and Mn-poor bands, the underlying pattern of segregation can be hidden behind a uniform martensite structure.
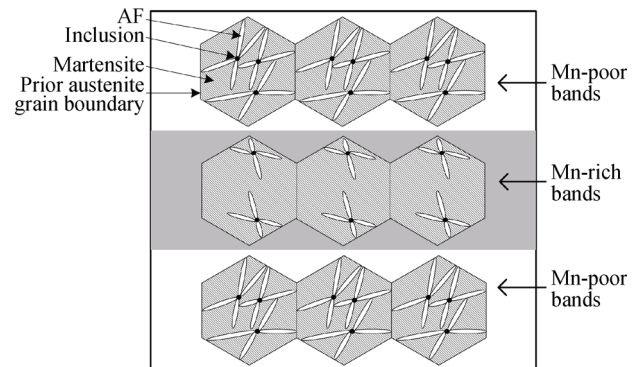

Fig. 10.   Schematic showing the formation mechanism of AF and martensite in segregated bands (less AF is formed in Mn-rich bands).
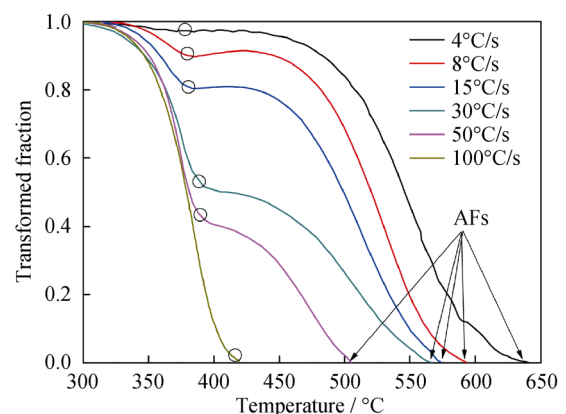

Fig. 11.   Obtained fractions of AF and martensite as a function of temperature for specimens with different cooling rates (martensite transformation is indicated by circles).

5. Conclusions

(1) For the isothermal transformation process, the speci-

men isothermed at 550°C exhibited a banded structure of AF and martensite because of the retardation of the AF transformation in Mn-rich bands. The specimen isothermed at 450°C was composed of single AF because a lower isothermal temperature is associated with a larger driving force, which permits AF to form even in Mn-rich regions.

(2) With respect to the continuous cooling process, the specimens cooled at rates from 4 to 50°C/s contained a mixture of AF and martensite in both segregated bands. For a given cooling rate, the martensite fraction in Mn-rich bands was always higher than that in Mn-poor bands because of the inhibiting effect of Mn enrichment on the AF formation.

(3) Increased cooling rates resulted in a less distinct AF-containing banded structure because accelerated cooling cause a smaller difference between AF nucleation rates in Mn-rich and Mn-poor bands.

Acknowledgements

References

[1] B.H. Chen and H. Yu, Hot ductility behavior of V–N and V–Nb microalloyed steels, *Int. J. Miner. Metall. Mater.*, 19(2012), No. 6, p. 525.

[2] F. Popa, I. Chicinaş, D. Frunză, I. Nicodim, and D. Banabic, Influence of high deformation on the microstructure of low-carbon steel, *Int. J. Miner. Metall. Mater.*, 21(2014), No. 3, p. 273.

[3] Y.M. Kim, H. Lee, and N.J. Kim, Transformation behavior and microstructural characteristics of acicular ferrite in line-pipe steels, *Mater. Sci. Eng. A*, 478(2008), No. 1-2, p. 361.

[4] I. Madariaga, I. Gutierrez, C.G. de Andrés, and C. Capdevila, Acicular ferrite formation in a medium carbon steel with a two stage continuous cooling, *Scripta Mater.*, 41(1999), No. 3, p. 229.

[5] A.M. Zhao, Y. Wang, Y.L. Chen, D. Tang, X.T. Gao, and B.Q. Zuo, Precipitation behaviors of X80 acicular ferrite pipeline steel, *Int. J. Miner. Metall. Mater.*, 18(2011), No. 3, p. 309.

[6] I.A. Yakubtsov and J.D. Boyd, Effect of alloying on microstructure and mechanical properties of bainitic high strength plate steels, *Mater. Sci. Technol.*, 24(2008), No. 2, p. 221.

[7] M.W. Zhou and H. Yu, Effects of precipitates and inclusions on the fracture toughness of hot rolling X70 pipeline steel plates, *Int. J. Miner. Metall. Mater.*, 19(2012), No. 9, p. 805.

[8] M.S. Joo, D.W. Suh, and H.K.D.H. Bhadeshia, Mechanical anisotropy in steels for pipelines, *ISIJ Int.*, 53(2013), No. 8, p. 1305.

[9] J.A. Eckert, P.R. Howell, and S.W. Thompson, Banding and the nature of large, irregular pearlite nodules in a hot-rolled low-alloy plate steel: a second report, *J. Mater. Sci.*, 28(1993), No. 16, p. 4412.

[10] J.D. Verhoeven, A review of microsegregation induced banding phenomena in steels, *J. Mater. Eng. Perform.*, 9(2000), No. 3, p. 286.

[11] R.A. Grange, Effect of microstructural banding in steel, *Metall. Trans.*, 2(1971), No. 2, p. 417.

[12] F García Caballero, A. García-Junceda, C. Capdevila, and C. García de Andrés, Evolution of microstructural banding during the manufacturing process of dual phase steels, *Mater. Trans.*, 47(2006), No. 9, p. 2269.

[13] G. Krauss, Solidification, segregation, and banding in carbon and alloy steels, *Metall. Mater. Trans. B*, 34(2003), No. 6, p. 781.

[14] F. D'Errico, Failures induced by abnormal banding in steels, *J. Failure Anal. Preven.*, 10(2010), No. 5, p. 351.

[15] T.F. Majka, D.K. Matlock, and G. Krauss, Development of microstructural banding in low-alloy steel with simulated Mn segregation, *Metall. Mater. Trans. A*, 33(2002), No. 6, p. 1627.

[16] K.S. McGarrity, J. Sietsma, and G. Jongbloed, Characterisation and quantification of microstructural banding in dual-phase steels: Part 2. Case study extending to 3D, *Mater. Sci. Technol.*, 28(2012), No. 8, p. 903.

[17] A. From and R. Sandström, Assessment of banding in steels by using advanced image analysis, *Mater. Charact.*, 41(1998), No. 1, p. 11.

[18] W. Xu, P.E.J. Rivera-Díaz-del-Castillo, and S. van der Zwaag, Ferrite/pearlite band prevention in dual phase and TRIP steels: model development, *ISIJ Int.*, 45(2005), No. 3, p. 380.

[19] B. Krebs, L. Germain, A. Hazotte, and M. Gouné, Banded structure in Dual Phase steels in relation with the austenite-to-ferrite transformation mechanisms, *J. Mater. Sci.*, 46(2011), p. 7026.

[20] F.G. Caballero, C. Garcia-Mateo, M.J. Santofimia, M.K. Miller, and C. García de Andrés, New experimental evidence on the incomplete transformation phenomenon in steel, *Acta Mater.*, 57(2009), No. 1, p. 8.

[21] J. Wang, P.J. Van Der Wolk, and S. Van Der Zwaag, On the influence of alloying elements on the bainite reaction in low alloy steels during continuous cooling, *J. Mater. Sci.*, 35(2000), No. 17, p. 4393.

[22] H.K.D.H. Bhadeshia, A rationalisation of shear transformations in steels, *Acta Metall.*, 29(1981), No. 6, p. 1117.

[23] K. Wu, Z. Li, A. Guo, X. L. He, L. Zhang, A. Fang, and L. Cheng, Microstructure evolution in a low carbon Nb–Ti microalloyed steel, *ISIJ Int.*, 46(2006), No. 1, p. 161.

[24] M. Calcagnotto, D. Ponge, and D. Raabe, On the effect of manganese on grain size stability and hardenability in ultrafine-grained ferrite/martensite dual-phase steels, *Metall. Mater. Trans. A*, 43(2012), No. 1, p. 37.

[25] M. Chang and H. Yu, Kinetics of bainite-to-austenite transformation during continuous reheating in low carbon microalloyed steel, *Int. J. Miner. Metall. Mater.*, 20(2013), No. 5, p. 427.